RSC Pharmaceutics

ROYAL SOCIETY OF CHEMISTRY

PAPER

View Article Online
View Journal | View Issue

Cite this: *RSC Pharm.*, 2024, **1**, 1055

Effect of fluorine substituents in 4-(1-benzyl-1*H*-benzo[*d*]imidazol-2-yl)thiazole for the study of antiparasitic treatment of cysticercosis on a *Taenia crassiceps* model†

Monserrath I. Rodríguez-Mora,[a] Raúl Colorado-Peralta,[b] Viviana Reyes-Márquez,[c] Marco A. García-Eleno,[d] Erick Cuevas-Yáñez,[d] Jesús R. Parra-Unda,[e] Abraham Landa[f] and David Morales-Morales *[a]

Received 13th July 2024,
Accepted 28th October 2024

DOI: 10.1039/d4pm00210e

rsc.li/RSCPharma

This work details the synthesis of five *N*-benzylated derivatives of thiabendazoles (**L1–L5**), four of which were previously unreported in the literature (**L2–L5**). The compounds were characterised using a comprehensive array of spectroscopic (FT-IR, ^{1}H, ^{13}C{1H}, and ^{19}F{1H} NMR), spectrometric (MS-EI+) and diffractometric (SC-DRX) techniques. To evaluate the effect of increased fluorine substituents in the *N*-benzyl fragment, we conducted a parasitotoxic activity assay, testing the compounds at various concentrations of unhatched *Taenia crassiceps* cysticerci. The inclusion of the *N*-benzyl fragment and the increase in fluorine substituents led to an enhancement in the lipophilicity of thiabendazoles.

Introduction

Benzimidazoles are bicyclic heteroaromatic compounds that have attracted the scientific community's attention since their introduction as antiparasitic agents in the 1960s.[1,2] These heterocyclic pharmacophores serve as essential scaffolds in designing new molecules with biological activity or clinical application. Benzimidazoles are among the ten most used nitrogenous heterocycles in medicines approved by the U.S. Food and Drug Administration (FDA), both in human and animal medicine, due to their notable pharmacological properties.[3,4] These compounds are capable of accepting or donating protons, allowing the formation of weak interactions, which promotes the union of the therapeutic targets with these heterocycles. Structure–activity relationship (SAR) analyses indicate that the placement of substituents in the N1, C2, C5 or C6 positions influences their therapeutic activity.[5,6] Modifications in benzimidazoles affect their binding capacity with proteins since new weak interactions and new electronic and steric effects arise, which alter their ability to recognise specific enzymes and modify their pharmacological potential.[7,8] These molecules have a structure similar to those of the nitrogenous bases known as purines (adenine and guanine), which facilitates their application in various biological activities, such as analgesic, anticancer, anticoagulant, anticonvulsant, antidiabetic, antihypertensive, antihistaminic, anti-inflammatory, antimalarial, antimicrobial, antioxidant, antipsychotic, antituberculosis, antitumor, antiulcer, antiviral, and contraceptive activities, among others.[9–11]

One of the best-known benzimidazoles is 4-(1*H*-benzo[*d*]imidazol-2-yl)thiazole, commonly called thiabendazole (TBZ). This compound inhibits the helminth-specific mitochondrial enzyme (fumarate reductase), which is why it is used as an anthelmintic agent in animals and humans.[12,13] TBZ was the first benzimidazole-based drug approved by the FDA for treating human gastrointestinal parasites. Even so, it was later withdrawn from the market because other anthelmintic agents with better tolerance emerged.[14,15] Nonetheless, this drug is still available in many countries and is mainly used in veterin-

[a]*Instituto de Química, Universidad Nacional Autónoma de México, Circuito Exterior S/N, C.P. 04510, Ciudad de México, Mexico. E-mail: damor@unam.mx*
[b]*Facultad de Ciencias Químicas, Universidad Veracruzana, Prolongación de Oriente 6, No. 1009, C.P. 94340, Orizaba, Veracruz, Mexico*
[c]*Departamento de Ciencias Químico-Biológicas, Universidad de Sonora, Luis Encinas y Rosales s/n, C.P. 83000, Hermosillo, Sonora, Mexico*
[d]*Centro Conjunto de Investigación en Química Sustentable UAEM-UNAM, Universidad Autónoma del Estado de México, Carretera Toluca-Atlacomulco Km. 14.5, C.P. 50200, Toluca, Estado de México, Mexico*
[e]*Unidad de Investigación en Salud Pública, Facultad de Ciencias Químico Biológicas, Universidad Autónoma de Sinaloa, Ave. de las Américas y Blvd. Universitarios, Ciudad Universitaria, C.P. 80100, Culiacán, Sinaloa, Mexico*
[f]*Departamento de Microbiología y Parasitología, Facultad de Medicina, Universidad Nacional Autónoma de México, Circuito Exterior S/N, Ciudad de México, C.P. 04510, Ciudad de México, Mexico*

†Electronic supplementary information (ESI) available: Full experimental details. CCDC 2350919–2350921. For ESI and crystallographic data in CIF or other electronic format see DOI: https://doi.org/10.1039/d4pm00210e

ary medicine. TBZ is also used as a fungicide and an anthelmintic in fruits, vegetables, and various food products.[16,17] This compound generally has low toxicity; however, the U.S. Environmental Protection Agency (EPA) has classified it as a probable carcinogen at doses high enough to cause disturbances in thyroid hormone balance.[18,19]

Brown and co-workers (1961) reported the preparation of 4-(1-benzyl-1*H*-benzo[*d*]imidazol-2-yl)thiazole (BZ-TBZ) when searching for a new class of broad-spectrum anthelmintic agents against gastrointestinal parasites of domestic animals. For this, TBZ was functionalised in the N1 position using benzoyl iodide.[20] Several studies have been reported on synthesising and characterising this TBZ derivative.[21–23] Even SAR experimental studies have been reported on its antimicrobial, anti-inflammatory and antiangiogenic activities, and as a vascular disruptor and methionine aminopeptidase inhibitor.[24–29]

On the other hand, *Taenia crassiceps* is a cestode found in wild canids and rodents. This parasite presents metabolic and antigenic similarities to different species of the *Taeniidae* family, such as *Taenia solium*, which makes it useful as an experimental model in cysticercosis studies.[30,31] Human cysticercosis caused by *Taenia crassiceps* is unusual; however, isolated cases have been reported in immunocompromised and immunocompetent patients.[32,33] One of the primary drugs used in the treatment of this disease is albendazole (ABZ), a derivative of benzimidazole. Nonetheless, parasite resistance to this drug has been reported, which has motivated the search for new alternatives for treating cysticercosis.[34,35] Thus, developing new benzimidazole derivatives aims to increase antiparasitic activity by slightly modifying traditional anthelmintics.[36,37] New compounds have been synthesised from 2-(trifluoromethyl)-1*H*-benzo[*d*]imidazole, presenting improved antiparasitic activity. For instance, 6-chloro-5-(2,3-dichlorophenoxy)-2-(trifluoromethyl)-1*H*-benzo[*d*]imidazole (RCB15) and 6-chloro-5-(naphthalen-1-yloxy)-2-(trifluoromethyl)-1*H*-benzo[*d*]imidazole (RCB20) have been chosen as promising molecules for the treatment of this disease, Scheme 1. These fluorinated benzimidazole derivatives had a greater effect on *Taenia crassiceps* cysticerci than ABZ and albendazole sulfoxide (ABZ-SO).[38,39] Therefore, this work reports the synthesis and characterisation of BZ-TBZ derivatives with different degrees of fluorination in the *N*-benzylic arm to study their effect on antiparasitic activity.

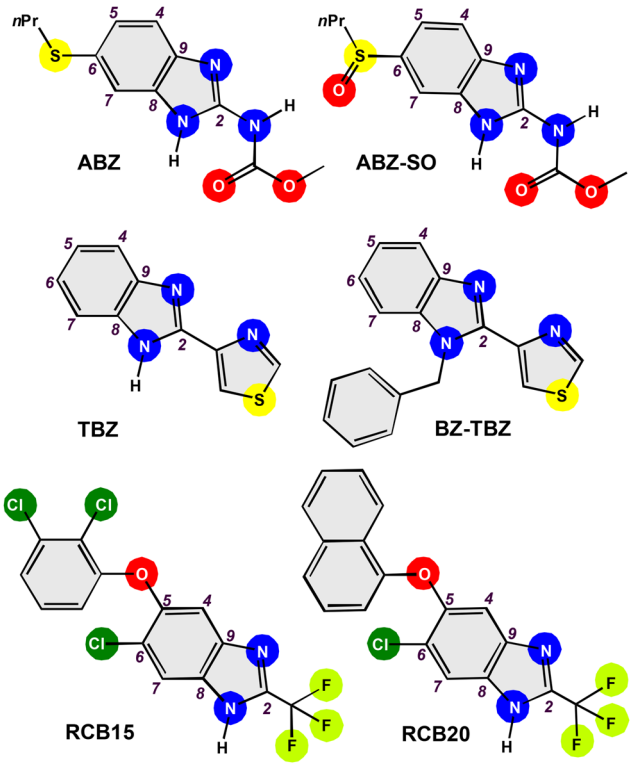

Scheme 1 Benzimidazole derivatives with anticysticercosis activity.

Materials and methods

Experimental details

All starting materials were purchased from commercial suppliers and used without further purification. The reagents employed were thiabendazole, sodium hydride 90%, benzyl bromide 98%, 3-fluorobenzyl chloride 96%, potassium iodide 99%, 2,3,6-trifluorobenzyl bromide 97%, 2,3,4,5,6-pentafluorobenzyl bromide 99%, and 4-(trifluoromethyl)benzyl bromide 98%. Melting points were determined directly using a Fisherbrand™ digital apparatus (open capillary). Infrared spectra were obtained using an FT-IR Bruker Alpha ATR spectrophotometer. The ^{1}H, $^{13}C\{^{1}H\}$ and $^{19}F\{^{1}H\}$ NMR experiments were carried out by using Bruker Avance III 300 MHz equipment using $CDCl_3$ in 5 mm tubes, and subsequently, the spectra were processed using MestReNova© software. Chemical shift values (δ) are reported in parts per million (ppm) relative to the internal reference (TMS). Mass spectra were recorded using a Jeol JSM-SX102A spectrometer at 10 kV in the EI+ mode. The colourless prismatic crystals were placed in a Bruker Smart Apex II X-ray diffractometer with a molybdenum X-ray source (λ = 0.71073 Å). The structures were solved and refined using Patterson's methods with the programs SHELXS-2014/7 and SHELXL-2019/2.[40] Molecular structures and supramolecular arrangements were analysed using Mercury© software. Additional information on structural data collection, resolution, and refinement can be found in the ESI.† The three structural files were deposited at the Cambridge Crystallographic Data Center (CCDC). The assigned deposit numbers for **L1**, **L2**, and **L4** were 2350921, 2350919, and 2350920,† respectively. Table 1 contains the crystallographic parameters, and Tables S1–S3† contain the distances and bond angles.

Synthesis of *N*-benzylated compounds

The compounds (**L1–L5**) were synthesised from the deprotonation of thiabendazoles (1 mmol, 0.2013 g) in the presence of sodium hydride (1 mmol, 0.0222 g). Subsequently, the product

Table 1 Crystal data and structure refinement for **L1**, **L2** and **L4**

	L1	L2	L4
Empirical formula	$C_{17}H_{13}N_3S$	$C_{17}H_{12}FN_3S$	$C_{17}H_8F_5N_3S$
Formula weight	291.36	309.36	381.32
Temperature	298(2) K	298(2) K	298(2) K
Wavelength	0.71073 Å	0.71073 Å	0.71073 Å
Monoclinic crystal system	Monoclinic	Monoclinic	Monoclinic
Space group	$P2_1/n$	$P2_1/n$	$P2_1/c$
Unit cell dimensions	a = 17.3372(8), α = 90° b = 9.2800(4), β = 113.263(2)° c = 19.3163(8), γ = 90°	a = 13.1322(4) Å, α = 90° b = 6.0454(2) Å, β = 107.2870(10)° c = 19.1953(7) Å, γ = 90°	a = 17.173(4) Å, α = 90° b = 8.1616(18) Å, β = 93.871(5)° c = 10.976(3) Å, γ = 90°
Volume	2855.1(2) Å^3	1455.07(8) Å^3	1534.8(6) Å^3
Z	8	4	4
Density (calculated)	1.356 Mg m^{-3}	1.412 Mg m^{-3}	1.650 Mg m^{-3}
Absorption coefficient	0.223 mm^{-1}	0.232 mm^{-1}	0.273 mm^{-1}
F(000)	1216	640	768
Crystal size	0.387 × 0.243 × 0.066 mm^3	0.462 × 0.167 × 0.090 mm^3	0.280 × 0.180 × 0.150 mm^3
Theta range for data collection	2.028 to 25.328°	1.673 to 25.390°	2.377 to 25.472°
Index ranges	$-20 \le h \le 20$, $-11 \le k \le 10$, $-23 \le l \le 22$	$-15 \le h \le 15$, $-7 \le k \le 7$, $-23 \le l \le 23$	$-20 \le h \le 20$, $-9 \le k \le 9$, $-13 \le l \le 13$
Reflections collected	25 355	12 341	13 161
Independent reflections	5207 [R(int) = 0.0919]	2674 [R(int) = 0.0421]	2837 [R(int) = 0.0851]
Completeness to theta	25.242°, 99.9%	25.242°, 100.0%	25.242°, 100.0%
Absorption correction	None	None	None
Refinement method	Full-matrix least-squares on F^2	Full-matrix least-squares on F^2	Full-matrix least-squares on F^2
Data/restraints/parameters	5207/0/379	2674/0/199	2837/608/357
Goodness-of-fit on F^2	0.903	0.967	0.958
Final R indices[I > 2sigma(I)]	R_1 = 0.0566, wR_2 = 0.1353	R_1 = 0.0344, wR_2 = 0.0791	R_1 = 0.0501, wR_2 = 0.1121
R indices (all data)	R_1 = 0.1475, wR_2 = 0.1725	R_1 = 0.0545, wR_2 = 0.0885	R_1 = 0.1201, wR_2 = 0.1392
Largest diff. peak and hole	0.354 and −0.397 e Å^{-3}	0.122 and −0.277 e Å^{-3}	0.164 and −0.246 e Å^{-3}

was reacted with each fluoro-substituted benzyl halide under a nitrogen atmosphere at the reflux of anhydrous tetrahydrofurans for 24 h. **L1** and **L3–L5** were obtained from fluoro-substituted benzyl bromides, while **L2** was obtained from 3-fluorobenzyl chloride and potassium iodide. The reactions were monitored by thin-layer chromatography (TLC) in a dichloromethane–methanol (95 : 5) mixture and developed using a UV lamp. Afterwards, the reaction products were purified by column chromatography and concentrated to dryness using a rotary evaporator connected to a high vacuum. **L1**, **L2** and **L4** crystallised from the slow evaporation of a mixture of dichloromethane with acetone.

4-(1-Benzyl-1*H*-benzo[*d*]imidazol-2-yl)thiazole (L1). It was synthesised from benzyl bromide (1 mmol, 0.1745 g). Light brown solid (0.2244 g, 77%). M.p. 146–148 °C. IR (ATR, ν cm^{-1}): 3111 (w), 3076 (w), 2916 (w), 1602 (w), 1450 (m), 1397 (m), 1303 (m), 1283 (w), 901 (m), 880 (m), 830 (m), 734 (s). ^{1}H NMR (300 MHz, $CDCl_3$, δ, ppm): 8.75 (s, 1H), 8.29 (s, 1H), 7.75 (d, 1H), 7.23–7.04 (m, 6H), 5.98 (s, 2H). ^{13}C{^{1}H} NMR (75 MHz, $CDCl_3$, δ, ppm): 153.07, 147.83, 146.96, 143.09, 137.11, 136.01, 128.71, 127.53, 126.74, 123.31, 122.87, 121.38, 119.79, 110.70, 48.54. MS-EI+ (m/z): 291, 214, 91.

4-(1-(3-Fluorobenzyl)-1*H*-benzo[*d*]imidazol-2-yl)thiazole (L2). It was synthesised from 3-fluorobenzyl chloride (1 mmol, 0.1506 g) and potassium iodide (1.5 mmol, 0.2515 g). White solid (0.2413 g, 78%). M.p. 140–142 °C. IR (ATR, ν cm^{-1}): 3122 (w), 3080 (w), 1614 (m), 1586 (m), 1480 (m), 1449 (m), 1437 (m), 1352 (w), 1295 (w), 1253 (w), 1141 (w), 939 (m), 829 (w), 746 (s). ^{1}H NMR (300 MHz, $CDCl_3$, δ, ppm): 8.78 (s, 1H), 8.27 (s, 1H), 7.75 (d, 1H), 7.25–7.09 (m, 4H), 6.86–6.76 (m, 3H), 5.98 (s, 2H). ^{19}F{^{1}H} NMR (282.77 MHz, $CDCl_3$, δ, ppm): −112.46. MS-EI+ (m/z): 309, 308, 214, 195, 135, 109.

4-(1-(2,3,6-Trifluorobenzyl)-1*H*-benzo[*d*]imidazol-2-yl)thiazole (L3). It was synthesised from trifluorobenzyl bromide (1 mmol, 0.2320 g). White solid (0.2590 g, 75%). M.p. 166–168 °C. IR (ATR, ν cm^{-1}): 3130 (w), 3030 (w), 3004 (w), 1493 (s), 1306 (m), 1242 (s), 1037 (m), 879 (w), 812 (m), 733 (s). ^{1}H NMR (300 MHz, $CDCl_3$, δ, ppm): 8.87 (s, 1H), 8.60 (s, 1H), 7.78 (d, 1H), 7.34 (d, 1H), 7.24 (dt, 2H), 6.97 (m, 1H), 6.71 (t, 1H), 6.34 (s, 2H). ^{19}F{^{1}H} NMR (282.77 MHz, $CDCl_3$, δ, ppm): −118.77, −136.53, −141.27. MS-EI+ (m/z): 345, 326, 214, 145.

4-(1-((Perfluorophenyl)methyl)-1*H*-benzo[*d*]imidazol-2-yl)thiazole (L4). It was synthesised from 2,3,4,5,6-pentafluorobenzyl bromide (1 mmol, 0.2636 g). White solid (0.2669 g, 70%). M.p. 150–152 °C. IR (ATR, ν cm^{-1}): 3122 (w), 3070 (w), 3002 (w), 2968 (w), 1657 (w), 1502 (s), 1400 (m), 1306 (m), 1120 (m), 948 (m), 821 (m), 732 (s). ^{1}H NMR (300 MHz, $CDCl_3$, δ, ppm): 8.85 (s, 1H), 8.50 (s, 1H), 7.77 (d, 1H), 7.28–7.19 (m, 3H), 6.33 (s, 2H). ^{19}F{^{1}H} NMR (282.77 MHz, $CDCl_3$, δ, ppm): −141.84, −153.09, −161.02. MS-EI+ (m/z): 381, 362, 303, 214, 181.

4-(1-(4-(Trifluoromethyl)benzyl)-1*H*-benzo[*d*]imidazol-2-yl)thiazole (L5). It was synthesised from 4-(trifluoromethyl)benzyl bromide (1 mmol, 0.2439 g). White solid (0.2803 g, 78%). M.p. 144–146 °C. IR (ATR, ν cm^{-1}): 3119 (w), 1619 (w), 1401 (s), 1100 (s), 1063 (s), 911 (m), 817 (m), 738 (s). ^{1}H NMR (300 MHz, $CDCl_3$, δ, ppm): 8.78 (s, 1H), 8.41 (s, 1H), 7.79 (d, 1H), 7.44 (d, 2H), 7.25 (m, 3H), 7.19 (d, 2H), 6.08 (s, 2H). ^{13}C{^{1}H} NMR (75 MHz, $CDCl_3$, δ, ppm): 153.16, 147.61, 146.79, 143.07,

141.21, 135.77, 126.94, 125.72, 123.54, 123.12, 121.56, 119.95, 110.28, 48.19. $^{19}F\{^{1}H\}$ NMR (282.77 MHz, $CDCl_3$, δ, ppm): −62.55. MS-EI+ (m/z): 359, 358, 214, 159.

Parasite viability *in vitro*

Taenia crassiceps strain Wake Forest University (WFU) cysticerci was obtained from the peritoneum of female BALB/cAnN mice at five months of intraperitoneal infection. Cysticerci were washed with sterile phosphate-buffered saline (PBS) and used for *in vitro* assays. The effect of parasitotoxic activity of **L1–L5** was determined on the viability and integrity of *Taenia crassiceps* cysticerci. To do this, seven groups of twenty parasites were incubated in microplates using Roswell Park Memorial Institute (RPMI) culture medium at 37 °C in 0.5% CO_2 for 24 h and analysed at 3, 6 and 24 h. Viability was evaluated with four different concentrations of the compounds (100, 200, 300, and 500 μM) compared to the same concentrations for the reference drugs, ABZ and TBZ. Subsequently, the parasites were incubated for 1 h in pig bile diluted at a 1 : 3 ratio with RPMI to observe evagination. Viability was estimated by evagination, contractile movements and damage to the bladder wall of the cysticerci, all observed under a Nikon Eclipse TS100 inverted microscope.

Results and discussion

Synthesis and structural characterisation

The *N*-benzylation reaction, a crucial step in our research, was performed at the N1 position of TBZ. This stage is fundamental in enhancing the lipophilicity and bioavailability of the new compounds, a key aspect of our study. This reaction also allowed the introduction of fluorine substituents on the *N*-benzylic arm in four of the five compounds. Therefore, **L1** and **L3–L5** were prepared by one-step synthesis, which consisted of reacting TBZ with different fluorinated benzyl bromides in the presence of sodium hydride under a nitrogen atmosphere. In the case of **L2**, 3-fluorobenzyl chloride was used in the presence of potassium iodide under the aforementioned conditions, Scheme 2. Most of the compounds recovered as white solids (**L2–L5**), except for **L1**, which was light brown. The compounds were obtained with yields between 70 and 78% and showed good solubility in common organic solvents, such as methanol, ethanol, acetone, dichloromethane, chloroform and dimethyl sulfoxide.

IR spectra provided the first evidence of the formation of the *N*-benzylated compounds. The absence of the signal due to the C–Br bond (ν = 650–515 cm^{-1}) from benzyl bromides indi-

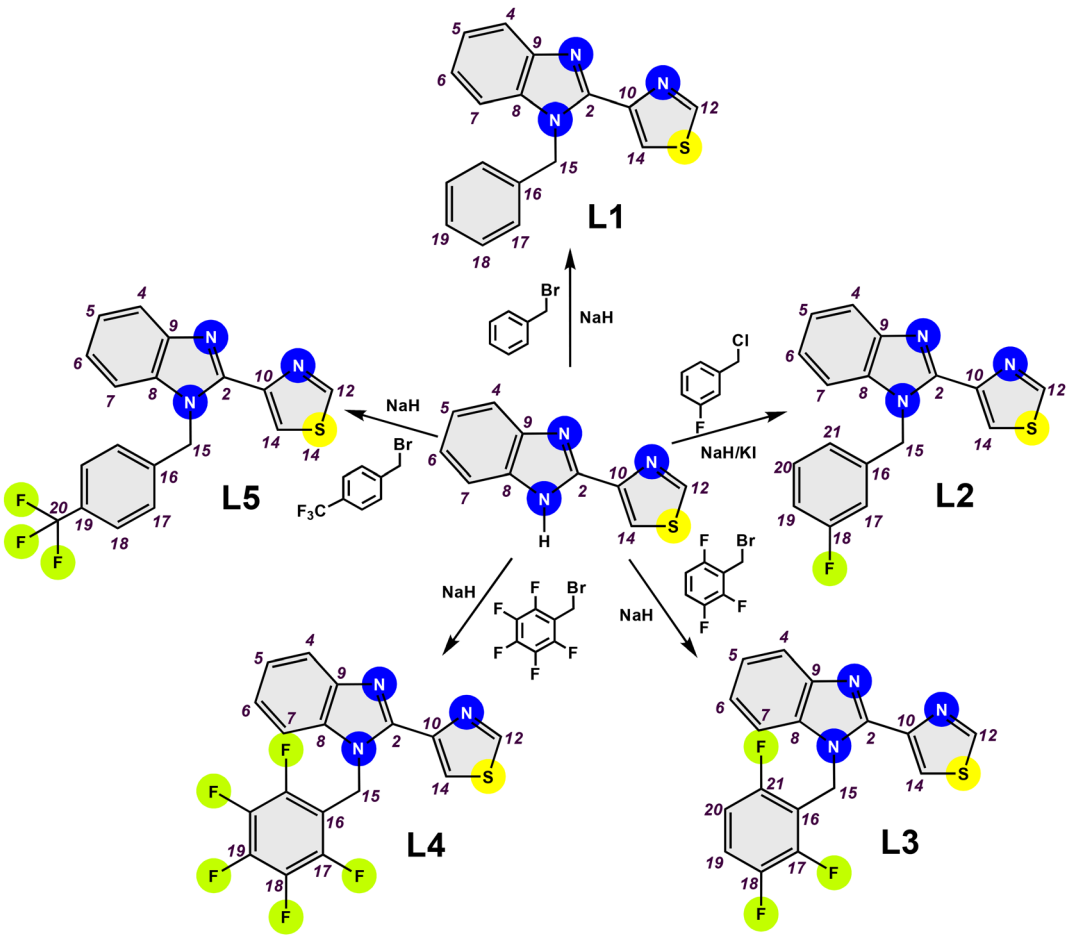

Scheme 2 General procedure for the preparation of fluorinated compounds derived from TBZ.

cated that the reaction had been completed. Besides, the absence of overtones in the spectra of each ligand (ν = 2800–2700 cm^{-1}) is an expected behaviour due to the lack of prototropic tautomerism of benzimidazole. The predictable peaks corresponding to the C=N, C–N and C–S bonds appeared at ν = 1657–1602 cm^{-1}, 1357–1310 cm^{-1} and 1141–1037 cm^{-1}, respectively, while the signal due to the C–F bond of the fluorinated rings in **L2–L4** was detected at ν = 948–911 cm^{-1}. The trifluoromethyl group in **L5** was detected at ν = 1100 cm^{-1}. In addition, the bands due to the aromatic C–H bond were observed at ν = 3130–3000 cm^{-1}, Fig. S1–S5.†

^{1}H NMR spectra showed evidence of *N*-benzylation, with the methylene signal assigned to the range of δ = 6.34–5.98 ppm (H15). For **L3** and **L4**, this same signal shifted to higher frequencies due to the greater number of fluorine substituents on the *N*-benzylic arm. The signals of thiazole rings appeared in the range of δ = 8.87–8.78 ppm (H12) and δ = 8.60–8.27 ppm (H14). The signals of the benzimidazole rings (H4–H7) and the *N*-benzyl fragment (H17–H21) overlapped in the aromatic region of δ = 7.80–6.68 ppm. In all cases, the H4 signal corresponds to a doublet in the range of δ = 7.80–7.74 ppm due to the absence of prototropic tautomerism in benzimidazole, Fig. S6–S10.†

In the $^{13}C\{^{1}H\}$ NMR spectra of **L1** and **L5**, the methylene carbon (C15) signal was assigned at 48.5 ppm for **L1** and 48.2 ppm for **L5**. The most displaced carbon in both compounds was the thiazole carbon (C12) due to its proximity to the nitrogen and sulphur heteroatoms (N11 and S13), at 153.1 ppm for **L1** and 153.2 ppm for **L5**. One of the most significant changes was observed in the quaternary benzyl carbon (C16) because it is found between the nitrogen atoms (N1 and N3), shifting from 137.1 ppm for **L1** to 141.2 ppm for **L5**. The coupling between ^{19}F and ^{13}C allowed the signals of the trifluoromethyl group to be assigned at 125.7 ppm (C20) and 129.6 ppm (C19), Fig. S11 and S12.†

Additionally, **L2–L5** were characterised by $^{19}F\{^{1}H\}$ NMR. The observed signals were consistent with the molecular structures proposed for the four fluorinated compounds. **L2** and **L5** presented a single signal. In the case of **L2**, the signal was observed at −112.5 ppm and corresponded to the fluorine atom placed in the *meta* position of the benzyl ring. In the case of **L5**, the signal was observed at −62.8 ppm and corresponded to the trifluoromethyl group placed in the *para* position of the benzyl ring. **L3** and **L4** exhibited the signals corresponding to the position of the fluorine atoms around the benzyl ring. For example, at −118.7, −136.5, and −141.3 ppm for **L3**, which correspond to the fluorine atoms placed at C17, C18 and C21, and at −141.8, −153.1 and −161.0 ppm for **L4**, which correspond to the fluorine atoms placed at C17, C19 and C18, respectively, Fig. S13–S16.† In the MS-EI+ data of **L1–L5**, the peak corresponding to the molecular ion of the five compounds was identified at *m*/*z* = 291, 309, 345, 381, 359. In addition, the fragment corresponding to TBZ was found at *m*/*z* = 214 for all compounds, Fig. S17–S21.†

Crystallographic analysis

The molecular structures of **L1**, **L2** and **L4** with an ellipsoid representation at a 50% probability level are presented in Fig. 1. **L1** presents two independent molecules in the asymmetric unit, crystallised in a monoclinic system with a *P*21/*n* space group with eight molecules in the unit cell. It is important to note that the benzimidazole ring approaches coplanarity with the thiazole ring with interplane angles of 9.68° and 14.91° between both molecules. In addition, the *N*-benzyl fragment has angles between planes of 83.95° and 88.01° between both molecules. On the other hand, **L2** crystallised in a monoclinic system with a *P*21/*n* space group with four molecules in the unit cell. Unlike **L1**, this compound crystallised with one molecule in the asymmetric unit. Furthermore, the presence of a fluorine atom in the meta position of the *N*-benzyl fragment can be observed. Finally, **L4** crystallised into a monoclinic system with a *P*21/*c* space with four molecules in the unit cell and one in the asymmetric unit. The N1 nitrogen atom bonds to the pentafluorobenzyl ring with an interplane angle of 74.20° concerning the benzimidazole ring. This compound presents disorder in the benzimidazole and thiazole rings.

In **L1**, the C20–H20···N3 hydrogen bond interactions stand out. These interactions can generate a 1D arrangement with an H20···N3 interaction distance of 2.60 Å ($\sum r_{vdW}$ = 2.75 Å) and a bond angle ∠C20–H20–N3 of 141°. The two molecules in the asymmetric unit are related by the interactions C25–H25···Cg1 and C31–H31···Cg1, forming a significant part of the molecular structure. The distances between the hydrogen atoms and the Cg1 centroid of the C16–C21 rings are 2.84 and 2.80 Å, respectively. The C–H···π interactions and the C20–H20···N3 hydrogen bond, perpendicular to each other, form a laminar arrangement parallel to the *ac* plane, Fig. 2. In **L2**, the N3 nitrogen atom of benzimidazole forms two C–H···N interactions, giving rise to a 1D arrangement along the *b*-axis. These arrangements present a distance of 2.55 and 2.74 Å ($\sum r_{vdW}$ = 2.75 Å) for C15–H15B···N3 and C14–H14···N3, respectively. The observed angle for ∠C15–H15B–N3 is 174°, and for the ∠C14–H14–N3 is 149°. In this same supramolecular arrangement, a C4–H4···S10 interaction is observed at a distance of 2.87 Å ($\sum r_{vdW}$ = 3.00 Å) with an angle ∠C4–H4–S10 of 156°. The arrangement is complemented by a π···π interaction between the benzimidazole's six-membered ring and the thiazole's five-membered ring with a distance of 3.772 Å between centroids. The complexity of the molecular arrangements is showcased in the 2D and 3D arrangements, which are stabilised by C–H···π interactions. For instance, the C19–H19···Cg1 interaction, together with the C–H···N interactions, generates a 2D arrangement parallel to the *bc* plane, Fig. 3. In **L4**, π···π interactions were found between the pentafluorinated system and the thiazole ring. The distance between the centroids was 3.74 Å, and these interactions stabilise the 3D supramolecular arrangement, Fig. 4.

Antiparasitic activity

Since 1979, when treatment with mebendazole (MBZ) at a single dose (50 mg kg^{-1} in rats) was shown to be effective in controlling infections caused by *Taenia crassiceps*,[41] multiple studies have been conducted to evaluate the effect of traditional drugs in the treatment of this disease. For example, it was proposed that combining praziquantel (PZQ) and ABZ-SO

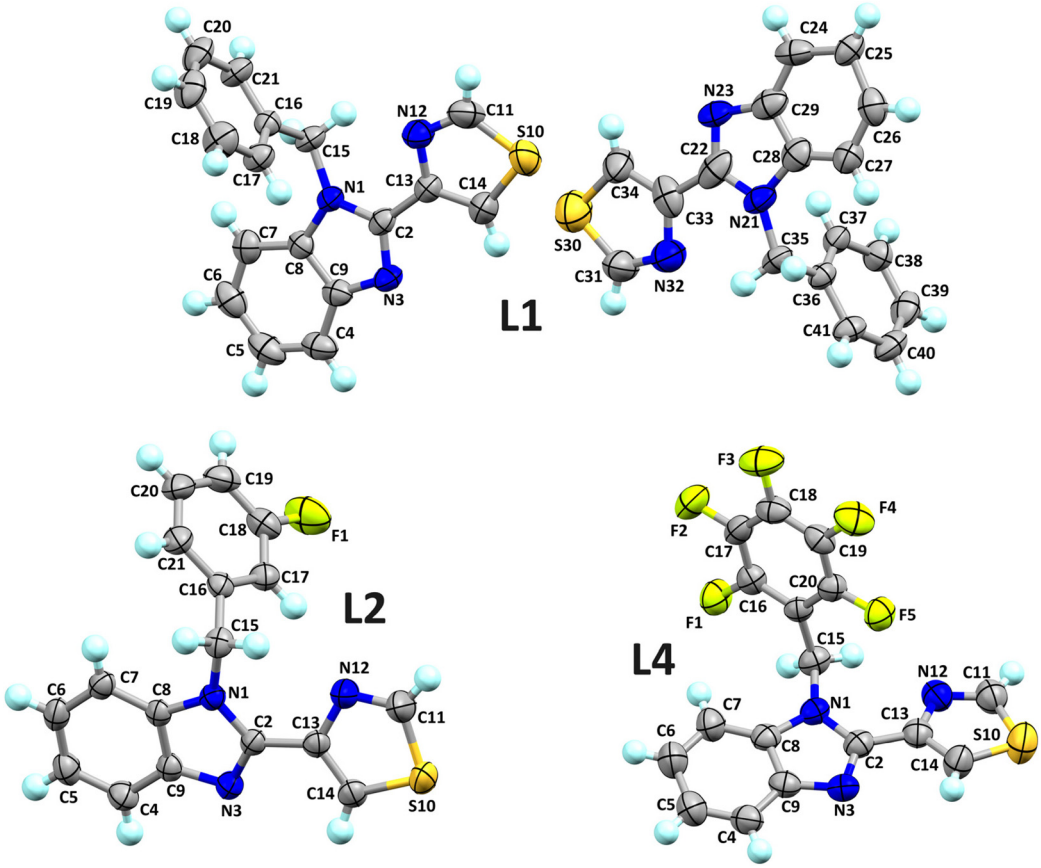

Fig. 1 Ellipsoidal representation at a 50% probability level of the molecular structures of **L1**, **L2** and **L4**.

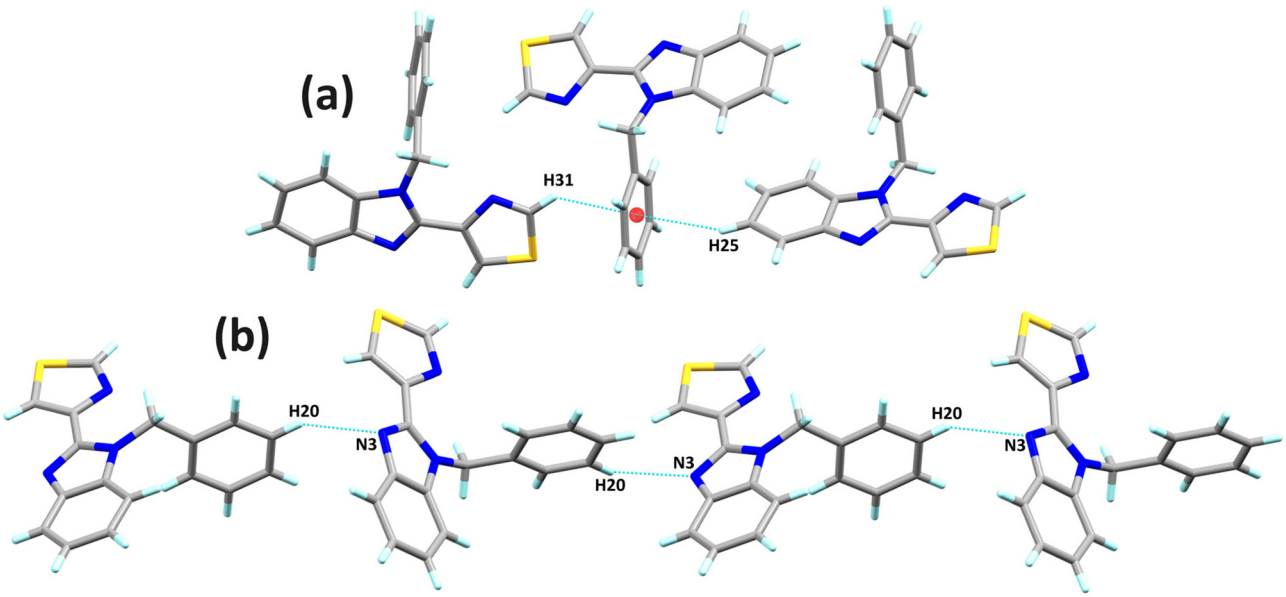

Fig. 2 (a) Lamellar arrangement of **L1** parallel to the *ac* plane, and (b) chain arrangement of **L1** generated by the C–H···N interaction.

could improve the current treatment of cysticercosis in a murine model with *Taenia crassiceps*.[42] This treatment was dependent on the exposure time and the concentration of both drugs.[43] In addition, the best time to start treatment was 10 days after infection and at least 20 days of treatment were required.[44] *In vitro* studies of the combination of nitazoxanide

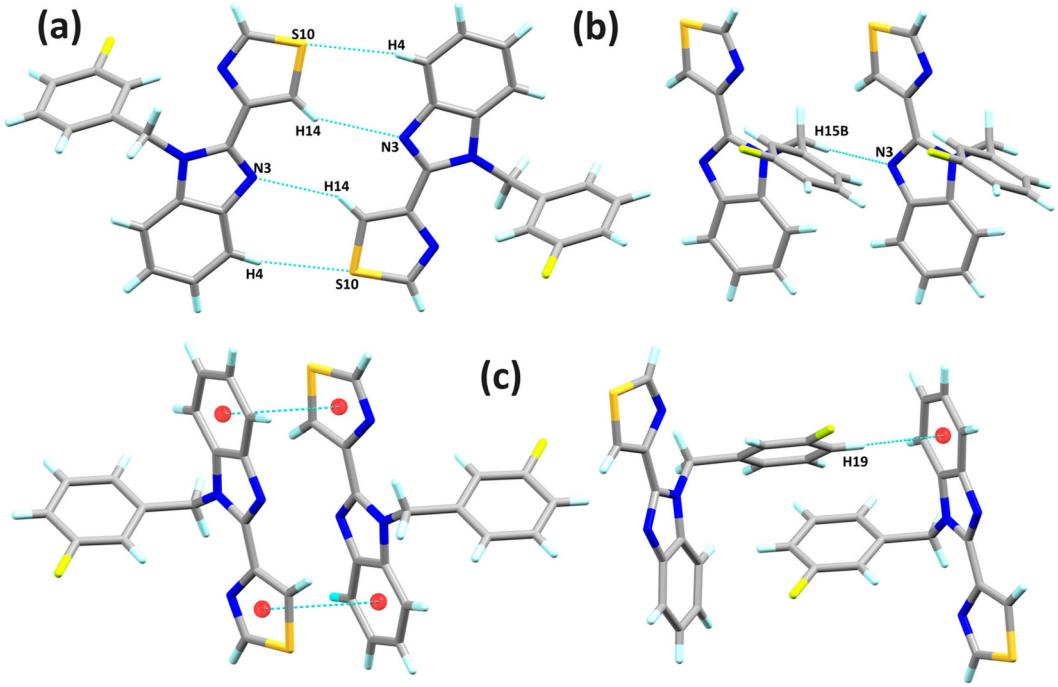

Fig. 3 (a) Dimeric arrangement of **L2** generated by the C–H···N and C–H···S interactions, (b) chain arrangement of **L2** generated by the C–H···N interaction, and (c) representation of the π···π and C–H···π interactions found in **L2**.

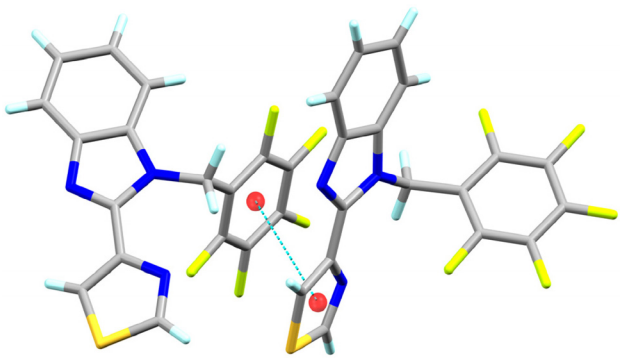

Fig. 4 Representation of the π···π interactions found between the pentafluorobenzyl and thiazole rings in **L4**.

(NTZ) with ABZ[45] or of NTZ and flubendazole (FLB) could be useful in the treatment of infections caused by *Taenia crassiceps* since they induce a greater metabolic impact on cysticerci compared to the isolated exposure of each of them.[46] Moreover, metabolic acidosis was greater in the group of cysticerci treated with NTZ than in the group treated with ABZ-SO, indicating that this is one of the modes of action used by this drug to induce parasite death.[47] NTZ induced stress in the energetic metabolism in the tricarboxylic acid cycle, in protein catabolism and in the oxidation of fatty acids in *Taenia crassiceps*, so it could be used as an alternative for the treatment of cysticercosis.[48] Additionally, other systems have been studied, such as curcumin oxidation products, which could act as suitable inhibitors of thioredoxin-glutathione reductase from *Taenia crassiceps* cysticerci.[49] As well as the ternary system ABZ-βCD-PVP (albendazole, β-cyclodextrin and polyvinylpyrrolidone) due to its greater dissolution, high bioavailability and better cysticidal activity with respect to ABZ.[50] Or, treatment with dehydroepiandrosterone (DHEA) which inhibits the establishment, growth and reproduction of *Taenia crassiceps* metacestodes.[51]

From the above, it is evident that most of the studies carried out for the treatment of cysticercosis in murine models with *Taenia crassiceps* have been carried out on drugs with a benzimidazole structure. Furthermore, it is known that evagination is a key indicator of the ability of the scolex to evaginate, a crucial process in the life cycle of *Taenia crassiceps*. Therefore, part of the methodology proposed by Parra-Unda and collaborators was used to evaluate the antiparasitic activity of compounds **L1–L5**.[52] This test is particularly relevant to this study as it helps understand the compounds' impact on the parasite's ability to develop and survive. In this context, the group incubated with ABZ at a concentration of 500 μM showed that after 24 h of incubation, 70% of evaginated cysticerci presented high mobility, but their integrity was reduced from complete to moderate. In the group incubated with TBZ, the percentage of evaginated cysticerci was 100% at the four exposure concentrations, and no reduction in integrity or mobility was observed. The cysticerci were only reduced in size by increasing the incubation time from 24 to 48 h with TBZ. In the five groups of parasites incubated with each of the five compounds, the percentage of evaginated cysticerci was 100%

Table 2 Effect of **ABZ**, **TBZ** and **L1–L5** (100, 200, 300 and 500 μM) on *Taenia crassiceps* cysticerci cultured in RPMI at 24 h

	ABZ	TBZ	L1	L2	L3	L4	L5
Control	[E] 100% [M] ++++ [D] C	[E] 100% [M] ++++ [D] C	[E] 100% [M] ++++ [D] C	[E] 100% [M] ++++ [D] C	[E] 100% [M] ++++ [D] C	[E] 100% [M] ++++ [D] C	[E] 100% [M] ++++ [D] C
EtOH/DMSO (0.5%)	[E] 100% [M] ++++ [D] C	[E] 100% [M] ++++ [D] C	[E] 100% [M] ++++ [D] C	[E] 100% [M] ++++ [D] C	[E] 100% [M] ++++ [D] C	[E] 100% [M] ++++ [D] C	[E] 100% [M] ++++ [D] C
100 μM	[E] 85% [M] ++++ [D] C	[E] 100% [M] ++++ [D] C	[E] 100% [M] ++++ [D] C	[E] 100% [M] ++++ [D] C	[E] 100% [M] ++++ [D] C	[E] 100% [M] ++++ [D] C	[E] 100% [M] ++ [D] C
200 μM	[E] 80% [M] ++++ [D] C	[E] 100% [M] ++++ [D] C	[E] 100% [M] ++++ [D] C	[E] 100% [M] ++++ [D] C	[E] 100% [M] ++++ [D] C	[E] 100% [M] ++++ [D] C	[E] 100% [M] + [D] C
300 μM	[E] 75% [M] ++++ [D] C	[E] 100% [M] ++++ [D] C	[E] 100% [M] ++++ [D] C	[E] 100% [M] ++++ [D] C	[E] 100% [M] ++++ [D] C	[E] 100% [M] + [D] C	[E] 100% [M] – [D] C
500 μM	[E] 70% [M] ++++ [D] M	[E] 100% [M] ++++ [D] C	[E] 100% [M] + [D] C	[E] 100% [M] + [D] C	[E] 100% [M] +++ [D] C	[E] 100% [M] – [D] C	[E] 100% [M] – [D] C

Viability was determined by: [E] percentage of evaginated cysticerci: number of evaginated parasites/total number of cultured parasites. [M] Parasite mobility: high (++++), medium (+++), moderate (++), low (+), and null (–). [D] Damage to the cysticerci wall: complete (C), medium (M) and null (N). Cysticerci cultured in RPMI medium were used as a control. Additionally, cysticerci were exposed to 0.5% DMSO for the ABZ assay and 0.5% absolute ethanol for the TBZ and **L1–L5** assays.

at any of the concentrations tested. Nonetheless, all compounds reduced the mobility of cysticerci with increasing concentration. **L4** and **L5** annulled mobility after 24 h of treatment at concentrations of 500 μM and 300 μM, respectively. A special case was the result obtained after 24 hours of incubation with **L1** at a concentration of 500 μM, observing 100% of evaginated but wrinkled cysticerci with low mobility. This could be because *N*-benzylation increases the partition coefficient, promoting a species with greater bioavailability but without action on mobility. **L4**, with the highest amount of fluorine substituents in the *N*-benzyl fragment, presented greater activity at a lower concentration compared to **L1–L3** but lower compared to **L5**. The steric volume and electron density of fluorine atoms in **L4** could be a critical factor in the interaction with phenylalanine of parasitic β-tubulin. **L5**, with the trifluoromethyl group in the *para* position of the *N*-benzyl ring, presented a greater action at a concentration comparable to that of ABZ, which could be directly related to the cancellation of the parasites' mobility, preventing their transfer to the hatching zone. **L5** is an excellent candidate for future studies in the treatment of cysticercosis. This compound presents the trifluoromethyl group in its structure, a very important functional group in recent studies of the possible drugs RCB15 and RCB20, Table 2.

Ethics approval

All protocols were carried out in the animal facilities of the Facultad de Medicina Universidad Nacional Autónoma de Mexico, under controlled conditions of temperature (22 °C), a relative humidity of 50–60% and 12 h dark/light cycles, in strict accordance with the Official Mexican Norm for the Production, Care, and Use of Laboratory Animals (NOM-062-ZOO-1999) and the Guide for the Care and Use of Laboratory Animals of the National Institutes of Health, U.S.A. The project was also approved by the Internal Committee for the Care and Use of Laboratory Animals (CICUAL-020-CIC-2018) de la Facultad de Medicina, UNAM, Mexico.

Conclusions

Five compounds derived from TBZ with an *N*-benzyl arm functionalised with fluoride substituents were synthesised and characterised. Remarkably, four of the compounds, excluding **L1**, have not been previously reported, adding a significant element of novelty to our research, as confirmed by our query in CAS Scifinder^{n}. Crystals of **L1**, **L2** and **L4** suitable for characterisation by SC-XRD were obtained. The supramolecular arrangements of the three structures are mainly supported by C–H···N3 intermolecular interactions. In addition, other weak interactions are reported, such as C–H···S10, C–H···π and π···π. All compounds showed activity in the mobility of *Taenia crassiceps* cysticerci, especially **L4** and **L5**. The effect of ABZ on mobility, integrity and evagination was observed at different concentrations. ABZ is the drug of choice to treat neurocysticercosis, acting selectively on the cytoplasmic microtubules of the intestinal cells of the parasite. TBZ inhibits the fumarate reductase enzyme of some helminths other than *Taenia solium* and *Taenia crassiceps*. Thus, this investigation represents the first study against cysticercosis in a murine model with *Taenia crassiceps* using novel, non-commercial molecules.

Author contributions

M. I. Rodríguez-Mora: investigation, methodology and conceptualization. R. Colorado-Peralta: writing – original draft,

visualization and formal analysis. V. Reyes-Márquez: writing – original draft, visualization and formal analysis. M. A. García-Eleno: investigation, supervision, software and validation. E. Cuevas-Yáñez: investigation, supervision, software and validation. J. R. Parra-Unda: investigation, methodology, resources and data curation. A. Landa: investigation, methodology, resources and data curation. D. Morales-Morales: conceptualization, resources, funding acquisition, project administration, and writing – review and editing.

Data availability

The data supporting this article have been included as part of the ESI.†

Conflicts of interest

There are no conflicts to declare.

Acknowledgements

The authors appreciate the collaboration of the institutions UAEM, UAS, UNAM, UNISON, and UV, and are thankful for CONAHCYT's financial support through the SNII. A. L. is thankful for the financial support from DGAPA-UNAM PAPIIT-205422. D. M-M. gratefully acknowledges the generous financial support from DGAPA-UNAM PAPIIT IN223323 and CONAHCYT A1-S-033933.

References

1 M. Faheem, A. Rathaur, A. Pandey, V. K. Singh and A. K. Tiwari, A Review on the Modern Synthetic Approach of Benzimidazole Candidate, *ChemistrySelect*, 2020, **5**(13), 3981–3994, DOI: **10.1002/slct.201904832**.

2 C. S. W. Law and K. Y. Yeong, Benzimidazoles in Drug Discovery: A Patent Review, *ChemMedChem*, 2021, **16**(12), 1861–1877, DOI: **10.1002/cmdc.202100004**.

3 B. Pathare and T. Bansode, Review-biological active benzimidazole derivatives, *Results Chem.*, 2021, **3**, 100200, DOI: **10.1016/j.rechem.2021.100200**.

4 Y. T. Lee, Y. J. Tan and C. E. Oon, Benzimidazole and its derivatives as cancer therapeutics: The potential role from traditional to precision medicine, *Acta Pharm. Sin. B*, 2023, **13**(2), 478–497, DOI: **10.1016/j.apsb.2022.09.010**.

5 H. E. Hashem and Y. El Bakri, An overview on novel synthetic approaches and medicinal applications of benzimidazole compounds, *Arabian J. Chem.*, 2021, **14**(11), 103418, DOI: **10.1016/j.arabjc.2021.103418**.

6 I. Beltran-Hortelano, V. Alcolea, M. Font and S. Perez-Silanes, The role of imidazole and benzimidazole heterocycles in Chagas disease: A review, *Eur. J. Med. Chem.*, 2020, **206**, 112692, DOI: **10.1016/j.ejmech.2020.112692**.

7 R. Veerasamy, A. Roy, R. Karunakaran and H. Rajak, Structure-activity relationship analysis of benzimidazoles as emerging anti-inflammatory agents: an overview, *Pharmaceuticals*, 2021, **14**(7), 663, DOI: **10.3390/ph14070663**.

8 M. Sweeney, D. Conboy, S. I. Mirallai and F. Aldabbagh, Advances in the synthesis of ring-fused benzimidazoles and imidazobenzimidazoles, *Molecules*, 2021, **26**(9), 2684, DOI: **10.3390/molecules26092684**.

9 K. Wu, X. Peng, M. Chen, Y. Li, G. Tang, J. Peng, Y. Peng and X. Cao, Recent progress of research on anti-tumor agents using benzimidazole as the structure unit, *Chem. Biol. Drug Des.*, 2022, **99**(5), 736–757, DOI: **10.1111/cbdd.14022**.

10 A. C. G, R. Gondru, Y. Li and J. Banothu, Coumarin-benzimidazole hybrids: A review of developments in medicinal chemistry, *Eur. J. Med. Chem.*, 2022, **227**, 113921, DOI: **10.1016/j.ejmech.2021.113921**.

11 D.-S. Son, E.-S. Lee and S. E. Adunyah, The Antitumor Potentials of Benzimidazole Anthelmintics as Repurposing Drugs, *Immune Netw.*, 2020, **20**(4), e29, DOI: **10.4110/in.2020.20.e29**.

12 M. Devereux, D. O'Shea, A. Kellett, M. McCann, M. Walsh, D. Egan, C. Deegan, K. Kędziora, G. Rosair and H. Müller-Bunz, Synthesis, X-ray crystal structures and biomimetic and anticancer activities of novel copper(II) benzoate complexes incorporating 2-(4′-thiazolyl)benzimidazole (thiabendazole), 2-(2-pyridyl)benzimidazole and 1,10-phenanthroline as chelating nitrogen donor ligands, *J. Inorg. Biochem.*, 2007, **101**(6), 881–892, DOI: **10.1016/j.jinorgbio.2007.02.002**.

13 M. A. Alam, Chapter 1 - Thiazole, a privileged scaffold in drug discovery, in *Privileged Scaffolds in Drug Discovery*, ed. B. Yu, N. Li and C. Fu, Academic Press, 2023, pp. 1–19. DOI: **10.1016/B978-0-443-18611-0.00027-9**.

14 K. El Bourakadi, M. E. M. Mekhzoum, A. E. K. Qaiss and R. Bouhfid, Recent Advances in the Synthesis and Applications of Thiabendazole Derivatives: A Short Review, *Curr. Org. Chem.*, 2020, **24**(20), 2367–2377, DOI: **10.2174/1385272824999200922090947**.

15 S. Kumar, M. T. Patil, R. Kataria and D. B. Salunke, 11. Thiazole: A privileged scaffold in drug discovery, in *Chemical Drug Desing*, ed. G. K. Gupta and K. Vinod, Boston, Berlin, 2016, pp. 243–281. DOI: **10.1515/9783110368826-013**.

16 M. Budetić, D. Kopf, A. Dandić and M. Samardžić, Review of Characteristics and Analytical Methods for Determination of Thiabendazole, *Molecules*, 2023, **28**(9), 3926, DOI: **10.3390/molecules28093926**.

17 Q. Wu, Y. Li, C. Wang, Z. Liu, X. Zang, X. Zhou and Z. Wang, Dispersive liquid–liquid microextraction combined with high performance liquid chromatography–fluorescence detection for the determination of carbendazim and thiabendazole in environmental samples, *Anal. Chim. Acta*, 2009, **638**(2), 139–145, DOI: **10.1016/j.aca.2009.02.017**.

18 R. Igual-Adell, C. Oltra-Alcaraz, E. Soler-Company, P. Sánchez-Sánchez, J. Matogo-Oyana and D. Rodríguez-Calabuig, Efficacy and safety of ivermectin and thiabendazole in the treatment of strongyloidiasis, *Expert Opin. Pharmacother.*, 2004, **5**(12), 2615–2619, DOI: **10.1517/14656566.5.12.2615**.

19 C. Henriquez-Camacho, E. Gotuzzo, J. Echevarria, A. C. White Jr, A. Terashima, F. Samalvides, J. A. Pérez-Molina and M. N. Plana, Ivermectin versus albendazole or thiabendazole for *Strongyloides stercoralis* infection, *Cochrane Database Syst. Rev.*, 2016, **1**, CD007745, DOI: **10.1002/14651858.CD007745.pub3**.

20 H. D. Brown, A. R. Matzuk, I. R. Ilves, L. H. Peterson, S. A. Harris, L. H. Sarett, J. R. Egerton, J. J. Yakstis, W. C. Campbell and A. C. Cuckler, Antiparasitic drugs. IV. 2-(4′-Thiazolyl)benzimidazole, a new anthelmintic, *J. Am. Chem. Soc.*, 1961, **83**(7), 1764–1765, DOI: **10.1021/ja01468a052**.

21 J. A. Maynard, I. D. Rae, D. Rash and J. M. Swan, Reaction of 2-(4-thiazolyl)benzimidazole (thiabendazole) with alkyl halides, *Aust. J. Chem.*, 1971, **24**(9), 1873–1881, DOI: **10.1071/CH9711873**.

22 P. P. Mahulikar, N. S. Pawar, D. S. Dalat and P. P. Patil, Synthesis of N-alkyl-2-(4-thiazolyl)-1H-benzimidazole and N-acyl-2-(4-thiazolyl)-1H-benzimidazole derivatives, *Org. Chem.: Indian J.*, 2007, **3**(1), 34–36 **https://www.tsijournals.com/articles/synthesis-of-biologically-active-nalkyland-nacyl-24thiazolyl-1hbenzimidazoles.pdf**.

23 S.-Q. Zhu, Y.-L. Liu, H. Li, X.-H. Xu and F.-L. Qing, Direct and Regioselective C-H Oxidative Difluoromethylation of Heteroarenes, *J. Am. Chem. Soc.*, 2018, **140**(37), 11613–11617, DOI: **10.1021/jacs.8b08135**.

24 N. S. Pawar, D. S. Dalal, S. R. Shimpi and P. P. Mahulikar, Studies of antimicrobial activity of *N*-alkyl and *N*-acyl 2-(4-thiazolyl)-1*H*-benzimidazoles, *Eur. J. Pharm. Sci.*, 2004, **21**(2–3), 115–118, DOI: **10.1016/j.ejps.2003.09.001**.

25 L. Pan, N. Hang, C. Zhang, Y. Chen, S. Li, Y. Sun, Z. Li and X. Meng, Synthesis and biological evaluation of novel benzimidazole derivatives and analogs targeting the NLRP3 inflammasome, *Molecules*, 2017, **22**(2), 213, DOI: **10.3390/molecules22020213**.

26 C. Zhang, B. Zhong, S. Yang, L. Pan, S. Yu, Z. Li, S. Li, B. Su and X. Meng, Synthesis and biological evaluation of thiabendazole derivatives as anti-angiogenesis and vascular disrupting agents, *Bioorg. Med. Chem.*, 2015, **23**(13), 3774–3780, DOI: **10.1016/j.bmc.2015.03.085**.

27 Z. Garkani-Nejad and F. Saneie, QSAR study of benzimidazole derivatives inhibition on *escherichia coli* methionine aminopeptidase, *Bull. Chem. Soc. Ethiop.*, 2010, **24(3)**, 317–325, DOI: **10.4314/bcse.v24i3.60661**.

28 R. Schiffmann, A. Neugebauer and C. D. Klein, Metal-Mediated Inhibition of *Escherichia coli* Methionine Aminopeptidase: Structure-Activity Relationships and Development of a Novel Scoring Function for Metal-Ligand Interactions, *J. Med. Chem.*, 2006, **49**(2), 511–522, DOI: **10.1021/jm050476z**.

29 M. A. Altmeyer, A. Marschner, R. Schiffmann and C. D. Klein, Subtype-selectivity of metal-dependent methionine aminopeptidase inhibitors, *Bioorg. Med. Chem. Lett.*, 2010, **20**(14), 4038–4044, DOI: **10.1016/j.bmcl.2010.05.093**.

30 A. G. Lescano and J. Zunt, Chapter 27 - Other cestodes: sparganosis, coenurosis and *Taenia crassiceps* cysticercosis, *Handb. Clin. Neurol.*, 2013, **114**, 335–345, DOI: **10.1016/B978-0-444-53490-3.00027-3**.

31 K. Willms and R. Zurabian, *Taenia crassiceps*: *in vivo* and *in vitro* models, *Parasitology*, 2010, **137**(3), 335–346, DOI: **10.1017/S0031182009991442**.

32 J. Morales-Montor and C. Larralde, The role of sex steroids in the complex physiology of the host-parasite relationship: the case of the larval cestode of *Taenia crassiceps*, *Parasitology*, 2005, **131**(3), 287–294, DOI: **10.1017/S0031182005007894**.

33 M. C. Romano, R. A. Valdéz, A. L. Cartas, Y. Gómez and C. Larralde, Steroid hormone production by parasites: the case of *Taenia crassiceps* and *Taenia solium* cysticerci, *J. Steroid Biochem. Mol. Biol.*, 2003, **85**(2–5), 221–225, DOI: **10.1016/S0960-0760(03)00233-4**.

34 A. N. Peón, A. Espinoza-Jiménez and L. I. Terrazas, Immunoregulation by *Taenia crassiceps* and its antigens, *BioMed Res. Int.*, 2013, 498583, DOI: **10.1155/2013/498583**.

35 A. Márquez-Navarro, A. Pérez-Reyes, A. Zepeda-Rodríguez, O. Reynoso-Ducoing, A. Hernández-Campos, F. Hernández-Luis, R. Castillo, L. Yépez-Mulia and J. R. Ambrosio, RCB20, an experimental benzimidazole derivative, affects tubulin expression and induces gross anatomical changes in *Taenia crassiceps* cysticerci, *Parasitol. Res.*, 2013, **112**, 2215–2226, DOI: **10.1007/s00436-013-3379-2**.

36 C. M. Fraga, T. L. da Costa, A. M. de Castro, O. Reynoso-Ducoing, J. Ambrosio, A. Hernández-Campos, R. Castillo and M. C. Vinaud, Alternative energy production pathways in *Taenia crassiceps* cysticerci *in vitro* exposed to a benzimidazole derivative (RCB20), *Parasitology*, 2016, **143**(4), 488–493, DOI: **10.1017/S0031182015001729**.

37 C. M. Fraga, T. Luiza da Costa, A. M. de Castro, O. Reynoso-Ducoing, J. Ambrosio, A. Hernández-Campos, R. Castillo and M. C. Vinaud, A benzimidazole derivative (RCB20) *in vitro* induces an activation of energetic pathways on *Taenia crassiceps* (ORF strain) cysticerci, *Exp. Parasitol.*, 2017, **172**, 12–17, DOI: **10.1016/j.exppara.2016.11.002**.

38 G. de Andrade Picanço, N. Ferreira de Lima, C. M. Fraga, T. L. da Costa, E. Isac, J. Ambrosio, R. Castillo and M. C. Vinaud, A benzimidazole derivative (RCB15) *in vitro* induces the alternative energetic metabolism and glycolysis in *Taenia crassiceps* cysticerci, *Acta Trop.*, 2017, **176**, 288–292, DOI: **10.1016/j.actatropica.2017.08.022**.

39 G. de A. Picanço, N. F. Lima, D. S. M. M. Alves, C. M. Fraga, T. L. Costa, R. de S. Lino Junior, R. Castillo, A. Hernández-Campos, J. Ambrosio and M. C. Vinaud, Partial inhibition of the tricarboxylic acid cycle in *Taenia crassiceps* cysticerci after the *in vitro* exposure to a benzimidazole derivative (RCB15), *Acta Trop.*, 2020, **202**, 105254, DOI: **10.1016/j.actatropica.2019.105254**.

40 G. M. Sheldrick, Crystal structure refinement with SHELXL, *Acta Crystallogr., Sect. C: Struct. Chem.*, 2015, **71**(1), 3–8, DOI: **10.1107/S2053229614024218**.

41 D. D. Heath and S. B. Lawrence, A single oral treatment with mebendazole for the control of *Taenia crassiceps* larval infections in rats, *Int. J. Parasitol.*, 1979, **9**(1), 73–76, DOI: **10.1016/0020-7519(79)90070-5**.

42 F. Palomares, G. Palencia, J. R. Ambrosio, A. Ortiz and H. Jung-Cook, Evaluation of the efficacy of albendazole sulfoxide and praziquantel in combination on *Taenia crassiceps* cysts: *in vitro* studies, *J. Antimicrob. Chemother.*, 2006, **57**(3), 482–488, DOI: **10.1093/jac/dki484**.

43 F. Palomares, G. Palencia, R. Pérez, D. González-Esquivel, N. Castro and H. Jung-Cook, In Vitro Effects of Albendazole Sulfoxide and Praziquantel against *Taenia solium* and *Taenia crassiceps* Cysts, *Antimicrob, Agents Chemother.*, 2004, **48**(6), 2302–2304, DOI: **10.1128/aac.48.6.2302-2304.2004**.

44 F. Palomares-Alonso, G. Palencia Hernández, I. S. Rojas-Tomé, H. Jung-Cook and E. Pinzón-Estrada, Murine cysticercosis model: Influence of the infection time and the time of treatment on the cysticidal efficacy of albendazole and praziquantel, *Exp. Parasitol.*, 2015, **149**, 1–6, DOI: **10.1016/j.exppara.2014.12.002**.

45 F. Palomares-Alonso, J. C. Piliado, G. Palencia, A. Ortiz-Plata and H. Jung-Cook, Efficacy of nitazoxanide, tizoxanide and tizoxanide/albendazole sulphoxide combination against *Taenia crassiceps* cysts, *J. Antimicrob. Chemother.*, 2007, **59**(2), 212–218, DOI: **10.1093/jac/dkl463**.

46 N. Ferreira de Lima, G. de Andrade Picanço, T. L. Costa and M. C. Vinaud, *In vitro* metabolic stress induced by nitazoxanide and flubendazole combination in *Taenia crassiceps* cysticerci, *Exp. Parasitol.*, 2022, **238**, 108265, DOI: **10.1016/j.exppara.2022.108265**.

47 E. Isac, G. de A. Picanço, T. L. da Costa, N. F. de Lima, D. de S. M. M. Alves, C. M. Fraga, R. de S. Jr. Lino and M. C. Vinaud, Nitazoxanide induces *in vitro* metabolic acidosis in *Taenia crassiceps* cysticerci, *Exp. Parasitol.*, 2016, **171**, 17–22, DOI: **10.1016/j.exppara.2016.10.012**.

48 E. Isac, G. A. Picanco, T. L. Costa, N. F. Lima, D. S. M. M. Alves, C. M. Fraga, R. S. Jr. Lino and M. C. Vinaud, In vitro nitazoxanide exposure affects energetic metabolism of Taenia crassiceps, flubendazole combination in *Taenia crassiceps* cysticerci, *Exp. Parasitol.*, 2020, **208**, 107792, DOI: **10.1016/j.exppara.2019.107792**.

49 A. Guevara-Flores, J. J. Martínez-González, A. M. Herrera-Juárez, J. L. Rendón, M. González-Andrade, P. V. Torres Durán, R. G. Enríquez-Habib and I. P. del Arenal Mena, Effect of curcuminoids and curcumin derivate products on thioredoxin-glutathione reductase from *Taenia crassiceps* cysticerci, Evidence suggesting a curcumin oxidation product as a suitable inhibitor, *PLoS One*, 2019, **14**(7), e0220098, DOI: **10.1371/journal.pone.0220098**.

50 F. Palomares-Alonso, C. Rivas González, M. J. Bernad-Bernad, M. D. Castillo Montiel, G. Palencia Hernández, I. González-Hernández, N. Castro-Torres, E. Pinzón Estrada and H. Jung-Cook, Two novel ternary albendazole–cyclodextrin–polymer systems: Dissolution, bioavailability and efficacy against *Taenia crassi*ceps cysts, *Acta Trop.*, 2010, **113**(1), 56–60, DOI: **10.1016/j.actatropica.2009.09.006**.

51 J. A. Vargas-Villavicencio, C. Larralde and J. Morales-Montor, Treatment with dehydroepiandrosterone *in vivo* and *in vitro* inhibits reproduction, growth and viability of *Taenia crassiceps* metacestodes, *Int. J. Parasitol.*, 2008, **38**(7), 775–781, DOI: **10.1016/j.ijpara.2007.10.011**.

52 R. Parra-Unda, F. Vaca-Paniagua, L. Jiménez and A. Landa, Cu,Zn superoxide dismutase: Cloning and analysis of the *Taenia solium* gene and *Taenia* crassiceps cDNA, *Exp. Parasitol.*, 2012, **130**, 32–38, DOI: **10.1016/j.exppara.2011.10.002**.